Reports on Progress in **Physics**

PURPOSE-LED PUBLISHING™

LETTER • **OPEN ACCESS**

Uniqueness of glasses prepared via x-ray induced yielding

To cite this article: Jacopo Baglioni *et al* 2024 *Rep. Prog. Phys.* **87** 120503

OPEN ACCESS
IOP Publishing

Letters
Reports on Progress in Physics

Rep. Prog. Phys. **87** (2024) 120503 (9pp)
https://doi.org/10.1088/1361-6633/ad91df

Letter

Uniqueness of glasses prepared via x-ray induced yielding

Jacopo Baglioni[1,*], Alessandro Martinelli[1,4], Peihao Sun[1], Francesco Dallari[1], Fabian Westermeier[2], Michael Sprung[2], Gerhard Grübel[3] and Giulio Monaco[1,*]

[1] Department of Physics and Astronomy 'Galileo Galilei', University of Padova, Via F. Marzolo, 8 - 35131 Padova, Italy
[2] Deutsches Elektronen-Synchrotron DESY, Notkestraße 85, 22607 Hamburg, Germany
[3] European X-ray Free-Electron Laser Facility GmbH, Holzkoppel 4, Schenefeld, 22869, Germany

E-mail: jacopo.baglioni@phd.unipd.it and giulio.monaco@unipd.it

Received 29 August 2024, revised 14 October 2024
Accepted for publication 13 November 2024
Published 25 November 2024

Corresponding editor: Dr Lorna Brigham

Abstract

The yield point marks the beginning of plastic deformation for a solid subjected to sufficient stress, but it can alternatively be reached by x-ray irradiation. We characterize this latter route in terms of thermodynamics, structure and dynamics for a series of $GeSe_3$ chalcogenide glasses with different amount of disorder. We show that a sufficiently long irradiation at room temperature results in a stationary and unique yielding state, independent of the initial state of the glass. The glass at yield is more disordered and has higher enthalpy than the annealed glass, but its properties are not extreme: they rather match those of a glass instantaneously quenched from a temperature 20% higher than the glass-transition temperature. This is a well-known, key temperature for glass-forming liquids which marks the location of a dynamical transition, and it is remarkable that different glasses upon irradiation head all there.

Supplementary material for this article is available online

Keywords: glasses, yielding, x-rays, chalcogenide glasses

The interest for glasses has been growing continuously following the increasing awareness of their importance, both at the fundamental level and in countless technological applications [1].

In many practical uses, ranging from materials science and engineering applications to civil construction, the understanding of their response to stress and the possibility to predict the elasto-plastic transformation and the fracture point at high-stress levels are crucial. The complex rheology of soft amorphous materials is also strongly related to this topic, and is a key aspect in biophysics and soft matter applications [2]. However, the intrinsic structural disorder of glasses and the dependence of their properties on the preparation procedure and thermal history complicate considerably both theoretical and experimental investigations of the phenomenon [3] and

[4] Current Address: Laboratoire Charles Coulomb, Université de Montpellier, CNRS, 34095 Montpellier, France.
[*] Authors to whom any correspondence should be addressed.

make the progress in the field much slower than for crystalline materials [4].

In this context, the yielding transition holds a particular relevance and has been under investigation for decades [5–7]. Beyond the yield point a solid subjected to mechanical stress displays plastic response. There is now increasing evidence that plastic events in glasses appear in the form of shear transformation zones, which are localized particle rearrangements releasing the accumulated stress [8, 9].

The yielding transition takes place when the density of these plastic regions is such that they form system-spanning structures [10–12]. Numerical simulations of model glasses [13–15] demonstrated that yielding can be cast in the general framework of phase transitions. The degree of disorder in the initial glass, fixed, e.g. by the cooling rate used to quench the glass from the melt, is suggested to play a key role to characterize the properties of this transition [14, 16].

When yielding is mentioned, the typical association is with the response of a material to stress or strain, and the numerical works mentioned earlier simulate this situation. However, we have recently proposed that yielding can alternatively be reached via x-ray irradiation [17]. The density fluctuations probed at inter-atomic distances during irradiation clearly show a transition from a solid-like behavior in the low dose regime (short irradiation time) to a behavior that, at high doses, matches the response of a flowing (yielding) material. In these experiments, the point defects generated upon irradiation are suggested to play the role of shear transformation zones [17]. Similar phenomena have been observed in chalcogenide glasses subjected to visible or infrared irradiation [18, 19]. Glasses containing As, Se or S are particularly photosensitive: laser irradiation can lead to an athermal fluidization of the glass [20, 21], though the competition between purely photo-induced and thermal effects remains a delicate and difficult matter of investigation [22].

Exploiting the photosensitivity of chalcogenide glasses, we here explore the yielding transition in a series of $GeSe_3$ glasses upon x-ray irradiation. This allows us to characterize this new path to yielding not only in terms of the thermodynamic response at the macroscopic scale but also in terms of the structural and dynamical response at the atomic scale. The properties of the glass prepared via x-ray induced yielding turn out to be very peculiar, as described in the following.

1. Results

1.1. X-ray induced modifications

The atomic-scale structural and dynamical information on amorphous $GeSe_3$ under x-ray irradiation has been obtained by simultaneous x-ray diffuse scattering and x-ray photon correlation spectroscopy (XPCS) measurements. In this part of the study, we used a focused x-ray beam with a flux of $7 \times 10^{10}\,\mathrm{ph\,s^{-1}}$. Both techniques are based on the collection of the time dependence of the scattered x-ray intensity, $I(q,t)$, where the scattering vector $q = \frac{4\pi}{\lambda}\sin(\theta/2)$ is defined by the scattering angle, θ, and the x-ray wavelength, λ. We fixed the scattering angle to probe the scattering vector $q_m = 1.06\,\mathrm{Å}^{-1}$ in order to focus on the intermediate-range order around the Ge-sites [23, 24]. X-ray diffuse scattering is used to monitor the changes in the atomic structure at this length-scale; XPCS probes, instead, the atomic dynamics encoded in the intensity correlation function, $g_2(q,t)$ [25, 26] (see SI for more details).

The XPCS results for a $GeSe_3$ glass prepared by quenching to room temperature from the melt at a rate of $10\,\mathrm{K\,s^{-1}}$ are shown in figure 1(a). The measured $g_2(q,t)$ functions are reported after baseline (d) subtraction and normalization to their short-time value (c), see SI for more details. These functions decay on a timescale of a few seconds: this is the timescale for atomic displacements over inter-atomic distances. Given that the glass-transition temperature, T_g, of this glass is much higher than room temperature [27], the observed dynamics cannot be the spontaneous dynamics of the glass, which is expected to be ultra-slow, but is rather induced by the x-ray beam. We remark that this effect is *purely* photo-induced and that the beam-induced temperature increase is negligible, see SI for experimental verification. This is also the same effect already observed in silicate, borate, and other chalcogenide glasses [28–30]: the characteristic decay time of the $g_2(q,t)$ functions depends on the dose-rate, but still remains sensitive to the atomic network [31] and to its modifications upon irradiation [17]. As found in these previous studies, the x-ray beam also induces clear structural changes as reported in figure 1(b). These data show that, following a transient regime that lasts about 100 s, the glass reaches a *stationary* state where neither the structure nor the induced dynamics show any further change. This state has been identified as the yielding glass in a recent work [17]. We note that the existence of a stationary state has been reported in glasses for nuclear waste applications after heavy ion irradiation [32], and despite the different mechanisms involved with different ionizing radiation, it might bear similarities to our observations. Moreover, we find that the stationary state is *stable* at room temperature: if the x-ray beam is switched off for some time and then turned on again, the structure and dynamics of the glass remain unchanged. On the other hand, the initial state can be fully recovered after heating up the glass above T_g and then quenching it down to room temperature.

1.2. Effects of the preparation protocol of the initial glass

Next we focus on the transient regime up to the yielding point for a $GeSe_3$ glass melt-quenched to room-temperature at different cooling rates. In order to get a more detailed understanding of the x-ray induced transformation, we probe the glasses by fast differential scanning calorimetry (FDSC) as a function of the x-ray irradiation time employing a recently developed setup [33]. In this part of the study, we use a rather unfocused x-ray beam with an intensity of $9 \times 10^{11}\,\mathrm{ph\,s^{-1}}$ which can irradiate the entire sample probed by FDSC. The time required to reach the stationary state depends on the x-ray dose (energy per unit mass) delivered to the sample: using the unfocused

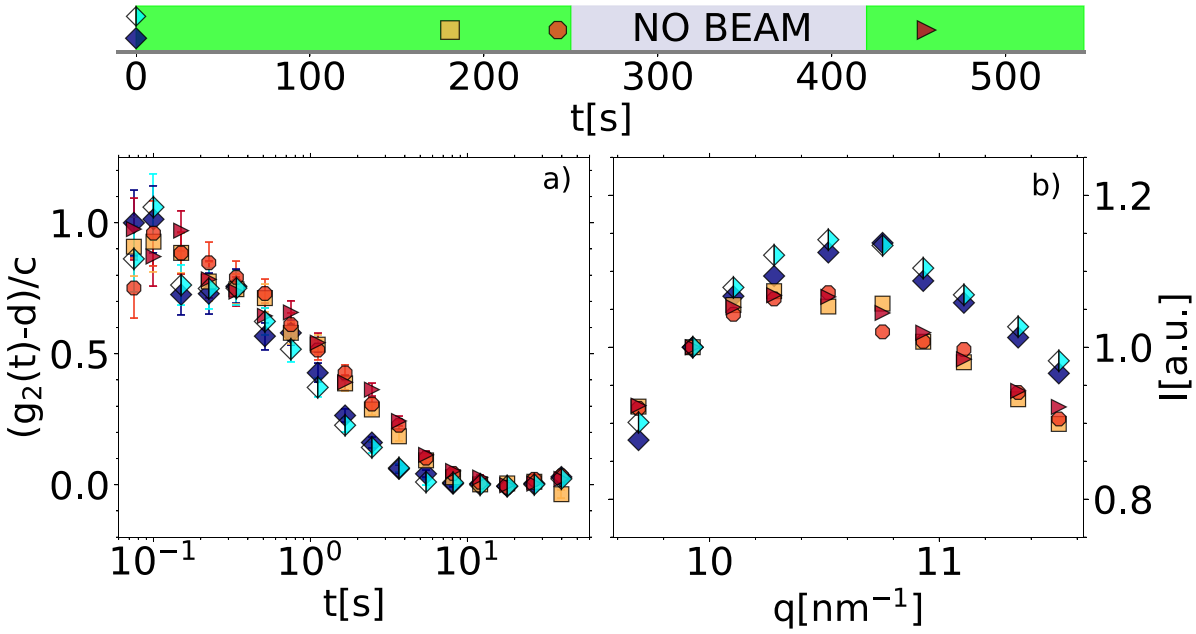

Figure 1. Stationarity and stability of a $GeSe_3$ glass at room temperature yielding upon x-ray irradiation. Atomic dynamics (a) and structure (b) of a $GeSe_3$ glass quenched at 10 K s^{-1}. In (a) the intensity correlation functions, $g_2(q,t)$, are reported after baseline [d] subtraction and normalization to their short-time value [c]. In (b) the x-ray scattered intensity is reported after normalization to the isosbestic point at 0.99 Å^{-1}. Full markers in blue, yellow, orange and red are associated with measurements taken on the same spot in the glass at times specified in the axis above the figures. Both dynamics and structure are stationary after ∼100 s of irradiation with the focused x-ray beam, see figure S8 in the SI for further details. The right pointing red triangles correspond to measurements taken on the same initial spot after a pause (with the x-ray beam off) and show that the glass reached by irradiation is stable. The half-light blue diamonds refer to measurements on the same spot but after heating up the sample above T_g and cooling it back to room temperature, and show that the pristine structure is thus recovered.

configuration, this time is longer than with the focused beam, see figure S7 in the SI for more details.

Figure 2 shows the FDSC traces (a) and the scattered intensity around the first sharp diffraction peak (b) for $GeSe_3$ glasses quenched at four different cooling rates. For each cooling rate, the measurements carried out at the start of the irradiation are compared with those corresponding to irradiation times sufficiently long to be in the stationary state. The stability of the pristine glasses (dashed lines in figure 2(a) can be inferred from the intensity of the enthalpy recovery peak appearing across the glass transition: the higher the enthalpy recovery peak, the higher the stability (the lower the enthalpy) of the pristine glass. The measurements performed after x-ray irradiation in the stationary state reveal that irradiation leads to a clear rejuvenation of the glass, i.e. to a state of higher enthalpy, and this is more evident for initially more stable glasses quenched at lower rates. At the quenching rate of 14 000 K s^{-1}, the glass is calorimetrically almost insensitive to x-ray irradiation. Similar trends can be observed in terms of scattered intensity, as shown in figure 2(b).

In particular, upon x-ray irradiation, we observe a reduction of the peak intensity and a shift of the peak position towards lower q-values. This behavior is qualitatively similar to the one observed in SiO_2 [28] and $LiBO_2$ [17]. However, the possibility to precisely control the cooling rate, and hence the stability of the initial glass, unveils a richer phenomenology. In fact, the changes induced by irradiation are stronger for initially more stable glasses, which is consistent with the FDSC results. The peak intensity reduction is an indication of increasing disorder at the intermediate length-scale [23, 24], consistent with the rejuvenation of the glass. The glass at yielding displays then both a higher enthalpy and increased disorder at the intermediate-range length-scale compared to its initial state. As a consequence, it will likely also display a more ductile mechanical response [34], though this remains to be verified.

1.3. Uniqueness of the yielding state

In figures 3(a) and (b), we compare the FDSC traces and scattering intensities in the pristine states and after reaching the yielding point. Remarkably, despite the significant differences for the initial states, the datasets overlap after reaching yielding. This suggests that, at yielding, the sample loses memory of its initial state and reaches a *unique* state in terms of enthalpy and structure at the intermediate length-scale.

We emphasize that the uniqueness of the yielding state refers here to the observation that this state is independent of the initial glass state and independent of the x-ray beam intensity/fluence, see figure S7 in the SI for experimental verification of this second point. However, the transition to the yielding state can still change (and will likely do) irradiating a glass at different temperatures, we will get back to this point later on. Also, given that the x-ray-induced changes of the thermodynamic and structural properties of the glass quenched at

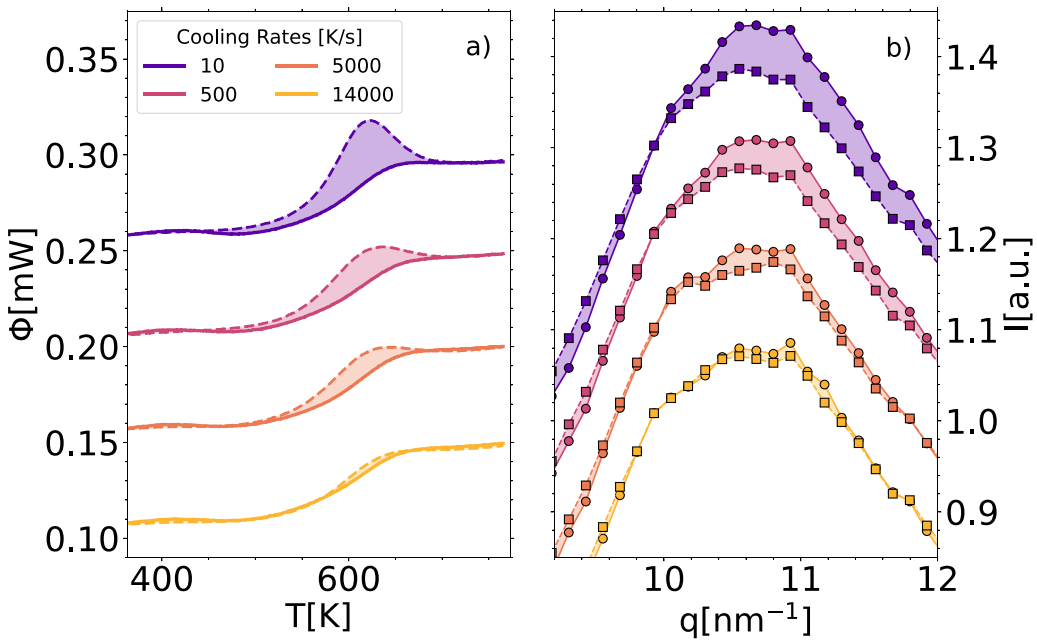

Figure 2. Effects of x-ray irradiation on $GeSe_3$ glasses quenched at different cooling rates. (a) Fast differential scanning calorimetry traces of $GeSe_3$ glasses as quenched (dashed lines) and at yielding (full lines). All curves have been measured with a probing rate of 2000 K s^{-1}. (b) X-ray scattered intensity around the first sharp diffraction peak at the start of irradiation (circles) and at yielding (squares). All curves, except the first from the bottom, are shifted by a constant with respect to the lower one: 0.05 mW in panel (a) and 0.1 in panel (b).

14 000 K s^{-1} are almost negligible, we can anticipate that the yielding state of $GeSe_3$ glasses irradiated with x-rays at room temperature is likely similar to a glass cooled down at that rate.

The FDSC traces measured as a function of cooling rate, r, and irradiation time (dose) can be used to compute the enthalpy of the corresponding glasses, and the results are shown in Figure 3(c). The enthalpy values have been all computed with respect to the same reference, see methods. The maximum enthalpy change upon irradiation amounts to $\sim$1.5 kJ mol^{-1}, similar to what was observed in bulk Ge–As–Se glasses upon sub-band-gap irradiation [35]. This is a remarkable enthalpy change, though comparable values are also reported in some organic glasses, e.g. in hyperquenched propylene glycol [36].

The data in figure 3(c) confirm quantitatively our observations above: the stationary glasses at yielding are iso-enthalpic, regardless of the enthalpy of the initial state. The increase in enthalpy as a function of irradiation time can be fitted with a stretched exponential function of the form:

$$\mathcal{H}(r,t) = \mathcal{H}_0(r) + \Delta\mathcal{H}_r(r)\left[1 - e^{(t/\tau)^\beta}\right], \qquad (1)$$

where $\mathcal{H}_0(r)$ and $\Delta\mathcal{H}_r(r)$ are the rate-dependent enthalpy of the pristine glass and the enthalpy change upon irradiation, respectively; τ and β are a characteristic time and a shape factor, respectively, which turn out to be independent of the rate and have the values $\tau = (69 \pm 5)$ s and $\beta = 0.53 \pm 0.02$. Moreover, the amplitude of the enthalpy variation $\Delta\mathcal{H}_r$ is directly related to the stability of the pristine glass: the lower is the cooling rate, the higher is the enthalpy variation induced by the x-ray beam.

Similarly, the intensity at the first sharp diffraction peak of the scattered radiation decreases to the same level for all glasses, see figure 3(d), and again according to a stretched exponential decay. The characteristic time and stretching coefficient that describe the dependence of the scattered intensity on the irradiation time are $\tau = (227 \pm 8)$ s and $\beta = 0.82 \pm 0.03$. The values of the relaxation time associated with enthalpy and intensity variations are close to each other (within a factor three), indicating that dynamic and thermodynamic modifications occur on comparable timescales.

Remarkably, these results bear strong qualitative similarities to numerical simulation results for glasses subjected to cyclic deformation [37]. Both upon irradiation and cyclic deformation, a glass reaches a unique yielding state independent of the properties of the initial glass. However, there is an important difference between these simulation results and our results here: while the sheared glasses undergo a clear first-order transition at yield, with a finite jump of the internal energy across a critical yield-strain, in our case the enthalpy changes across the yielding transition are continuous. Nonetheless, the results are not incompatible, because the yielding transition is reached through different paths: by increasing either the strain or the dose. In particular, when a glass is subjected to a slow shear deformation, plastic flow proceeds until yield via a sequence of sudden, localized flow events that take place at soft spots in the glassy matrix. In the case of x-ray irradiation explored here, instead, the sequence of flow events in the structure, initiated by the formation of point defects, is stochastic: it takes place at random positions in the network structure which

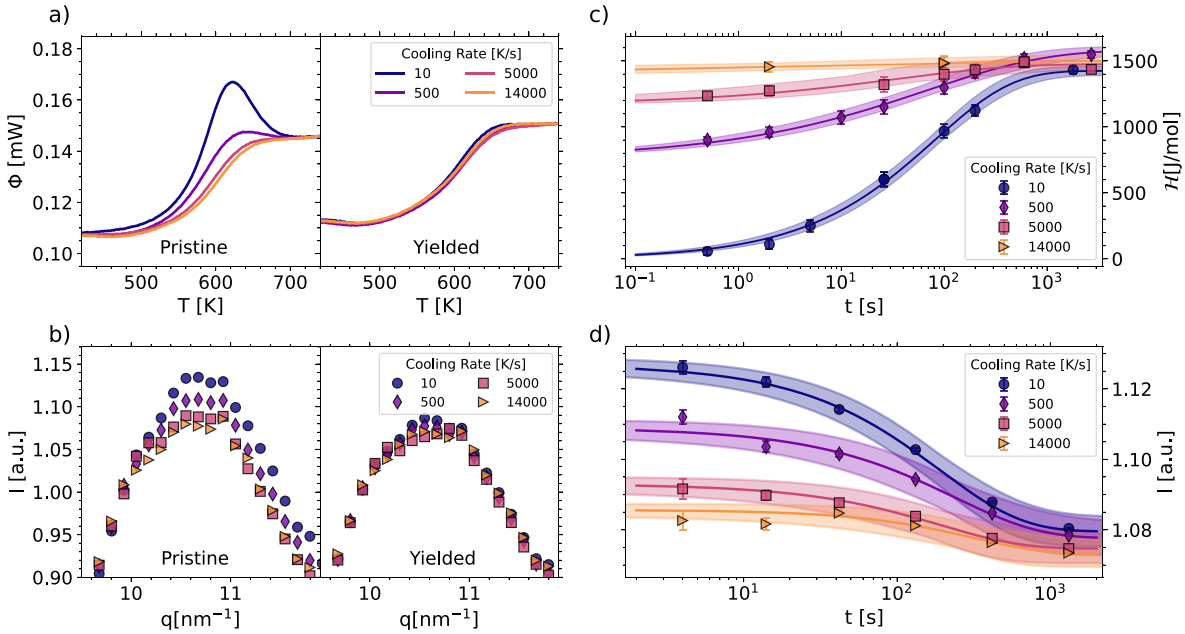

Figure 3. Structural and thermodynamic evolution of $GeSe_3$ glasses upon irradiation. (a) FDSC traces of the glasses as-prepared (left) and in the stationary state (right). (b) The corresponding patterns of the scattered intensity around the first sharp diffraction peak. (c) X-ray irradiation-time dependence of the enthalpy of $GeSe_3$ glasses quenched to room temperature at different cooling rates. The enthalpy values are computed with respect to the same reference, which is the glass prepared by cooling at $10\,\mathrm{K\,s^{-1}}$. Within errorbars, all glasses reach an iso-enthalpic state independently of their initial stability. (d) X-ray irradiation-time dependence of the x-ray scattered intensity at the first sharp diffraction peak for the same glasses as in (c). Also in this case, within errorbars, all irradiated glasses reach an iso-structural state independently of their initial stability.

are related to the random locations of x-ray absorption events. As such, the sequence of flow events in a glass upon x-ray irradiation seems more similar to what one would expect for a supercooled liquid in (metastable) equilibrium conditions.

2. Discussion

The observation that the characteristic time τ and the shape factor β that describe the enthalpy increase upon irradiation are independent of the initial glass has further implications. In fact, once the total enthalpy change is normalized, for each glass, to the maximum enthalpy change, $[\mathcal{H}(r,t) - \mathcal{H}_0(r)]/\Delta\mathcal{H}_r(r)$, a master curve is obtained, as shown in figure 4(a). This conclusion also holds for the intensity variations, see SI. In other words, the same time constant characterizes the approach to the yield point of a very stable glass as well as an unstable one. This can be understood if we consider that x-ray photoabsorption events take place randomly in the glass: the build-up of a network of point defects is expected to be described by the same characteristic amount of time regardless of the defect concentration at the beginning of the irradiation.

It is also interesting to understand what is so special about the yielding glass reached upon irradiation. To this aim, we compute for each measured FDSC trace, and therefore for each couple of cooling-rate/irradiation-time, the fictive temperature, $T_f(r,t)$, of the corresponding glass. This is a single parameter that captures important properties of the glass and that can be thought of as the temperature of the supercooled liquid which, instantaneously quenched, is isostructural to the glass [38]. In particular, we compute T_f following the method proposed in [39, 40], see SI for more details. In figure 4(b) the T_f values, normalized to the glass-transition temperature, T_g, are reported as a function of the irradiation time. It is interesting to observe that all glasses at yielding converge to a fictive temperature close to $1.2T_g$.

In other words, the yielding state reached upon irradiation by all $GeSe_3$ glasses at room-temperature has the same structure of the supercooled liquid at $1.2T_g$, suggesting significant, though not extreme, rejuvenation. A similar level of rejuvenation has been reported for ion-irradiated metallic glasses [41], which may be related to the phenomenology discussed here. While even more extreme rejuvenation of glasses has been achieved, e.g. by constrained loading in compression [42] or laser surface melting [43], the unique state that we reach here is consistent with the idea that the yielding glass follows a process of photoinduced fluidization.

Remarkably, the fictive temperature of the yielding glass is a very special temperature in glass-forming liquids: it is known as the mode-coupling temperature, T_c, and a dynamic cross-over takes place there [44]. It marks the temperature where the atomic dynamics changes from being diffusive at high temperature to being dominated by activated processes

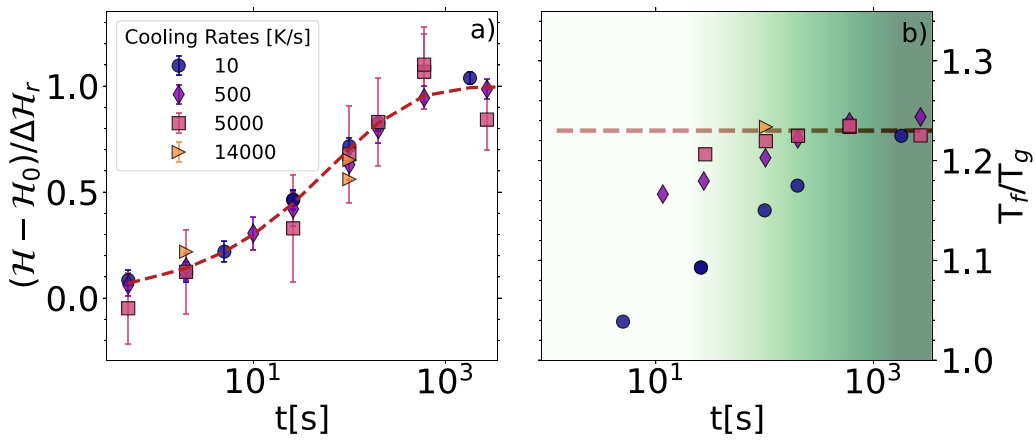

Figure 4. Nature of the yielding glass. (a) Enthalpy variations for glasses of different stability normalized to the maximum enthalpy variation as a function of the irradiation time. All curves collapse on a master curve. (b) Fictive temperature for the different studied glasses normalized to the glass-transition temperature, $T_g = 497$ K, as a function of the irradiation time. All glasses converge to the same fictive temperature of $\sim$1.2 T_g (dashed horizontal line).

at lower temperature: below T_c the system can be thought of hopping between different minima of its potential energy landscape [45–47]. A similar connection between the effective temperature of the yielding glass and T_c was recently made for a model glass studied in numerical simulations under shear [37]. The idea that a slowly driven solid, as in our case, is exploring phase space as a high temperature equilibrium liquid has also been discussed theoretically [48, 49]. Our results are experimental evidence of a link between the yielding state of a slowly driven glass and T_c: they strongly support the fundamental connection between driven glasses and supercooled liquids, which is a topic at the focus of current discussion [50].

As mentioned above, it should be stressed that the yielding state reached upon x-ray irradiation at room temperature is unique for $GeSe_3$ glasses.

However, the x-ray induced yielding transition will likely depend on the temperature of the glass. From this point of view, the x-ray-induced yielding transition explored here might bear similarities with the stress-induced glass-transition studied in computer simulations of metallic glasses [51]. In particular, for glasses irradiated at higher temperatures, thermal relaxation effects will set in and compete with purely photo-induced effects. At temperatures well below T_g the x-ray-induced yielding transition might be instead independent of the temperature of the glass. For the present case of $GeSe_3$ glasses, we are likely in this athermal limit (or close to it) given that room temperature is $\sim 0.5 T_g$. However, the x-ray induced yielding transition discussed here remains to be characterized in this respect.

Our results have also another implication that can be important for the development of novel glassy materials. The stationarity of the yielding glass here reported suggests that a glass in this state is stable upon further perturbation by irradiation, as here analyzed, or by mechanical deformation, as implied by the previous discussion of numerical simulation results [37].

Glasses at the yielding point should then be seriously considered for critical applications in presence of high levels of mechanical stress or in radiation-hostile environments.

3. Methods

3.1. Samples

The $GeSe_3$ glass was prepared starting from the pure elements (3N purity). The powders (total mass $\sim$5 g), mixed at the stoichiometric ratio, were inserted in a silica ampule previously cleaned with a mixture of sulfuric acid and hydrogen peroxide. The ampule was sealed in vacuum and heated up to 1273 K in a furnace. After 30 h, the sample was quenched in water at room temperature. Then, after an annealing of 6 h at $T = 493$ K, it was cooled down to room temperature at 30 K h^{-1}. Small pieces of the order of a few hundreds of ng were taken from the resulting rod and mounted on the membrane chip of a commercial calorimeter Flash DSC 2+ from Mettler Toledo. The sample was melted on the chip to ensure a good thermal contact and then cooled down to room temperature at the desired cooling rate. Melting the glass clearly erases its previous thermal history. The lateral extension of the sample size on the chip was $\sim 35\,\mu$m, and its thickness, estimated from x-ray transmission measurements, was $\sim 30\,\mu$m.

The protocol used to melt the sample on the chip, as well as all other temperature protocols used here, have been optimized to ensure that the sample composition remains stable. For example, the sample was melted on the chip heating it up to 773 K, a temperature well above the glass transition, and keeping it there for $\sim$1 ms. This is a long enough time to melt the sample but is short enough to ensure that no Se is lost by evaporation, as demonstrated by (i) the compatibility of the measured T_g with the one reported in the literature [23], and (ii) the fact that repeated cycles do not change neither T_g

nor the overall enthalpy of the sample, both of which would change in case of losses of Se.

3.2. Combined x-ray diffuse scattering and XPCS measurements

The details of the experimental setup employed here are discussed in [33]. In a nutshell, we integrated a commercial calorimeter Flash DSC 2+ from Mettler Toledo in the coherence beamline P10 at Petra III (DESY, Hamburg) [52]. This allows us to combine x-ray diffuse scattering and XPCS to study the interatomic-scale structure and dynamics, respectively, of a glass prepared at different quenching rates from the melt thanks to the fast response of the calorimeter. Here, the x-ray photon energy was set to 8.1 keV ($\lambda = 1.53$ Å), and the beam was focused to a spot of $3.3 \times 2.0\,\mu$m FWHM ($H \times V$). The x-ray beam intensity was 7×10^{10} ph s^{-1} corresponding, for our samples, to a dose-rate of $\sim$9 MGy s^{-1}. The details of the dose calculation can be found in the SI.

The sample (and the chip of the calorimeter) was kept in vacuum at room temperature. The x-rays scattered from the sample were collected in transmission geometry by an EigerX4M 2D detector (2167 [H] $\times$ 2070 [V] square pixels 75 μm in size) positioned at 1.8 m from the sample at a scattering angle of $\theta = 14°$. This angle corresponds to the first sharp diffraction peak of the scattered intensity of the glass [23], and thus the scattered intensity is particularly sensitive to the intermediate-range order around the Ge-sites [24]. Each measurement consisted of a series of scattered intensity patterns integrated from 10 ms to 25 ms each during periods ranging from 80 s to 250 s, and thus corresponding to series of the order of 10 000 frames per measurement. Each pattern was integrated over iso-q ROIs in order to provide series of q- and time-resolved intensities, $I(q,t)$. A single frame is sufficient to provide a statistically-robust scattered-intensity pattern, as shown in the main text.

The XPCS data result from the computation of the normalized intensity correlation functions, see SI for more details. The feasibility of XPCS measurements on the MEMS-sensor employed in chip-based calorimeters has been demonstrated recently for oxide and metallic glasses [33]. Here we use the same approach for $GeSe_3$ glasses. We positioned the sample in transmission geometry as the thickness of the glass melted on the chip is close to the absorption length of $GeSe_3$ (31 μm) at the x-ray energy used here, and the signal from the MEMS' membrane is negligible at the scattering angle investigated here. The XPCS measurements have been acquired with a focal spot size small enough to provide sufficient contrast in the intensity correlation function, the contrast being inversely proportional to the beam size [25]. After each measurement, and thus after each irradiation up to the yielding point of the glass, the sample was melted as discussed above to erase the memory of the previous irradiation; the sample was then cooled down again to room temperature at the chosen rate for a new acquisition, and the entire procedure was repeated several times to reach the desired statistics for the XPCS data.

3.3. Combined x-ray diffuse scattering and FDSC measurements

In order to study the structural and the thermodynamic responses of our glasses for different cooling rates and irradiation times until yielding, we combined x-ray diffuse scattering and FDSC. The setup was identical to the one described above, but the x-ray beam was focused to a spot of 98 μm $\times$ 93 μm FWHM ($H \times V$). In fact, a beam size larger than the lateral extension of the sample size is necessary to guarantee a uniform and complete irradiation of the glass and to study the photo-induced thermodynamic variation. The x-ray beam intensity was 9×10^{11} ph s^{-1} corresponding, for our samples, to a dose-rate of $\sim$0.4 MGy s^{-1}. The x-ray diffuse scattering patterns were collected as described above. The shape of the diffuse scattering peak does not change on changing the beam spot size in the range considered here. The scattered intensity in the two setups has been carefully calibrated in order to match on a single dose-rate scale the dynamical, structural and thermodynamic response, see SI for more details.

The FDSC traces have been acquired for glasses prepared at different cooling rates and exposed to the x-ray beam for different irradiation times. The chip has two identical cells as the calorimetric measurements are based on a differential approach. The FDSC traces report the heat release rate as a function of temperature. For each measurement we irradiated both the reference side and the sample for the same amount of time, leveraging the differential method to correct for any possible x-ray induced effects on the chip membrane. After each irradiation, the glass was probed at a heating rate of 2000 K s^{-1} up to 773 K, cooled down at the same rate, and cycled one more time with the same procedure in order to obtain a baseline for subtraction from the first cycle, see SI for more details. The temperature reported in the FDSC traces has been calibrated using as a reference the crystallization temperature of a piece of benzoic acid placed on top of the glass sample. For what concerns the analysis of the FDSC traces, we focus here on the enthalpy changes, i.e. on the integral of the difference of the traces measured in the first and second heating cycle. These values for the enthalpy changes have then been referred to a fixed reference, chosen to be the glass prepared by cooling from the melt at a rate of 10 K s^{-1}. These enthalpy values, denoted as $\mathcal{H}$, have then been used to characterize the effects of the preparation protocol (cooling rate) and irradiation time on the $GeSe_3$ glasses.

Data availability statement

The data that support the findings of this study are openly available at the following DOI: 10.25430/researchdata.cab.unipd.it.00001434.

Acknowledgments

This research was carried out at beamline P10 (Experiment 11017606 and long-term Project II-20210011EC) at DESY, a

member of the Helmholtz Association (HGF). J B acknowledges support by the Centre for Molecular Water Science (CMWS) in an Early Science Project. The research leading to this result has been supported by the Project GLAXES ERC-2021-ADG (Grant Agreement No. 101053167) funded by the European Union. Dr C Scian from the Physics and Astronomy Department of the University of Padova is gratefully acknowledged for his support in the preparation of the $GeSe_3$ sample.

Author contributions

J B, A M and G M designed the research; J B, A M, P S, F D, F W, M S and G M performed the research; J B analyzed the data; and J B and G M wrote the paper, with contributions from all authors.

ORCID iDs

Jacopo Baglioni https://orcid.org/0000-0003-0322-0941
Alessandro Martinelli https://orcid.org/0000-0002-4971-9986
Peihao Sun https://orcid.org/0000-0002-3608-1557
Francesco Dallari https://orcid.org/0000-0003-0171-8084
Fabian Westermeier https://orcid.org/0000-0003-0696-206X
Gerhard Grübel https://orcid.org/0000-0002-8633-8234
Giulio Monaco https://orcid.org/0000-0003-2497-6422

References

[1] Eggleton B J, Luther-Davies B and Richardson K 2011 Chalcogenide photonics *Nat. Photon.* **5** 141–8
[2] Bonn D, Denn M M, Berthier L, Divoux T and Manneville S 2017 Yield stress materials in soft condensed matter *Rev. Mod. Phys.* **89** 035005
[3] Hufnagel T C, Schuh C A and Falk M L 2016 Deformation of metallic glasses: recent developments in theory, simulations and experiments *Acta Mater.* **109** 375
[4] Rice J R and Thomson R 1974 Ductile versus brittle behavious of crystals *Phil. Mag.* **29** 73
[5] Nicolas A, Ferrero E E, Martens K and Barrat J-L 2018 Deformation and flow of amorphous solids: insights from elastoplastic models *Rev. Mod. Phys.* **90** 045006
[6] Berthier L, Biroli G, Manning M L and Zamponi F 2024 Yielding and plasticity in amorphous solids (arXiv:2401.09385)
[7] Aime S, Truzzolillo D, Pine D J, Ramos L and Cipelletti L 2023 A unified state diagram for the yielding transition of soft colloids *Nat. Phys.* **19** 1673–9
[8] Argon A S and Kuo H Y 1979 Plastic flow in a disordered bubble raft (an analog of a metallic glass) *Mater. Sci. Eng.* **39** 101
[9] Falk M L and Langer J S 1998 Dynamics of viscoplastic deformation in amorphous solids *Phys. Rev.* E **57** 7192–205
[10] Shi Y and Falk. M L 2005 Strain localization and percolation of stable structure in amorphous solids *Phys. Rev. Lett.* **95** 095502
[11] Cao P, Short M P and Yip S 2019 Potential energy landscape activations governing plastic flows in glass rheology *Proc. Natl Acad. Sci. USA* **116** 18790–7
[12] Ozawa M, Berthier L, Biroli G and Tarjus G 2022 Rare events and disorder control the brittle yielding of well-annealed amorphous solids *Phys. Rev. Res.* **4** 023227
[13] Jaiswal P K, Procaccia I, Rainone C and Singh M 2016 Mechanical yield in amorphous solids: a first-order phase transition *Phys. Rev. Lett.* **116** 085501
[14] Ozawa M, Berthier L, Biroli G, Rosso A and Tarjus G 2018 Random critical point separates brittle and ductile yielding transitions in amorphous materials *Proc. Natl Acad. Sci. USA* **115** 6656–61
[15] Sastry S 2021 Models for the yielding behavior of amorphous solids *Phys. Rev. Lett.* **126** 255501
[16] Rossi S, Biroli G, Ozawa M, Tarjus G and Zamponi F 2022 Finite-disorder critical point in the yielding transition of elastoplastic models *Phys. Rev. Lett.* **129** 228002
[17] Martinelli A, Caporaletti F, Dallari F, Sprung M, Westermeier F, Baldi G and Monaco G 2023 Reaching the yield point of a glass during x-ray irradiation *Phys. Rev.* X **13** 041031
[18] Popescu M A 2000 *Non-Crystalline Chalcogenides* (Kluwer Academic Publishers)
[19] Tanaka K and Shimakawa K 2011 *Amorphous Chalcogenide Semiconductors and Related Materials* (Springer)
[20] Hisakuni H and Tanaka K 1995 Optical microfabrication of chalcogenide glasses *Science* **270** 974–5
[21] Gueguen Y, Christophe Sangleboeuf J, Keryvin V, Lépine E, Yang Z, Rouxel T, Point C, Bureau B, Zhang X-H and Lucas P 2010 Photoinduced fluidity in chalcogenide glasses at low and high intensities: a model accounting for photon efficiency *Phys. Rev.* B **82** 134114
[22] Li L, Khanolkar A R, Ari J, Deymier P and Lucas P 2021 Origin of photoelastic phenomena in Ge-Se network glasses *Phys. Rev.* B **104** 214209
[23] Rowlands R F, Zeidler A, Fischer H E and Salmon P S 2019 Structure of the intermediate phase glasses $GeSe_3$ and $GeSe_4$: the deployment of neutron diffraction with isotope substitution *Front. Mater.* **6** 133
[24] Salmon P S, Martin R A, Mason P E and Cuello G J 2005 Topological versus chemical ordering in network glasses at intermediate and extended length scales *Nature* **435** 75
[25] Madsen A, Fluerasu A and Ruta B 2016 Structural dynamics of materials probed by XPCS *Synchrotron Light Sources and Free-Electron Lasers: Accelerator Physics, Instrumentation and Science Applications* (Springer) pp 1617–41
[26] Berne B J and Pecora R 1976 *Dynamic Light Scattering: With Applications to Chemistry, Biology and Physics* (Dover Publications)
[27] Gueguen Y, Rouxel T, Gadaud P, Bernard C, Keryvin V and Sangleboeuf J-C 2011 High-temperature elasticity and viscosity of Ge_xSe_{1-x} glasses in the transition range *Phys. Rev.* B **84** 064201
[28] Ruta B, Zontone F, Chushkin Y, Baldi G, Pintori G, Monaco G, Ruffle B and Kob W 2017 Hard x-rays as pump and probe of atomic motion in oxide glasses *Sci. Rep.* **7** 3962
[29] Pintori G, Baldi G, Ruta B and Monaco G 2019 Relaxation dynamics induced in glasses by absorption of hard x-ray photons *Phys. Rev.* B **99** 224206
[30] Li J, Madhavi M, Jeppson S, Zhong L, Dufresne E M, Aitken B, Sen S and Kukreja R 2022 Observation of collective molecular dynamics in a chalcogenide glass: results from x-ray photon correlation spectroscopy *J. Phys. Chem.* B **126** 5320–5
[31] Pintori G, Baldi G, Dallari F, Martinelli A, Sprung M and Monaco G 2022 X-ray induced dynamics in borate glasses with different network connectivity *Phys. Rev.* B **105** 104207
[32] Peuget S, Tribet M, Mougnaud S, Miro S and Jégou C 2018 Radiations effects in ISG glass: from structural changes to long-term aqueous behavior *npj Mater. Degrad.* **2** 23

[33] Martinelli A, Baglioni J, Sun P, Dallari F, Pineda E, Duan Y, Spitzbart-Silberer T, Westermeier F, Sprung M and Monaco G 2024 A new experimental setup for combined fast differential scanning calorimetry and x-ray photon correlation spectroscopy *J. Synchrotron Radiat.* **31** 557–65
[34] Kumar G, Neibecker P, Liu Y H and Schroers J 2013 Critical fictive temperature for plasticity in metallic glasses *Nat. Commun.* **4** 1536
[35] Calvez L, Yang Z and Lucas P 2008 Light-induced matrix softening of Ge–As–Se network glasses *Phys. Rev. Lett.* **101** 177402
[36] Wang Li-M, Borick S and Austen Angell C 2007 An electrospray technique for hyperquenched glass calorimetry studies: propylene glycol and di-*n*-butyl phthalate *J. Non-Cryst. Solids* **353** 3829–37
[37] Bhaumik H, Foffi G and Sastry S 2021 The role of annealing in determining the yielding behavior of glasses under cyclic shear deformation *Proc. Natl Acad. Sci. USA* **118** e2100227118
[38] Tool A Q 1946 Relation between inelastic deformability and thermal expansion of glass in its annealing range *J. Am. Ceram. Soc.* **29** 240–53
[39] Moynihan C T, Easteal A J, Ann De Bolt M and Tucker J 1976 Dependence of the fictive temperature of glass on cooling rate *J. Am. Ceram. Soc.* **59** 12–16
[40] Guo X, Potuzak M, Mauro J C, Allan D C, Kiczenski T J and Yue Y 2011 Unified approach for determining the enthalpic fictive temperature of glasses with arbitrary thermal history *J. Non-Cryst. Solids* **357** 3230–6
[41] Magagnosc D J, Kumar G, Schroers J, Felfer P, Cairney J M and Gianola D S 2014 Effect of ion irradiation on tensile ductility, strength and fictive temperature in metallic glass nanowires *Acta Mater.* **74** 165–82
[42] Pan J, Wang Y X, Guo Q, Zhang D, Greer A L and Li Y 2018 Extreme rejuvenation and softening in a bulk metallic glass *Nat. Commun.* **9** 560
[43] Greer A L 1995 Diffusion and reactions in thin films *Appl. Surf. Sci.* **86** 329
[44] Götze W 1999 Recent tests of the mode-coupling theory for glassy dynamics *J. Phys.: Condens. Matter* **11** A1
[45] Schrøder T B, Sastry S, Dyre J C and Glotzer S C 2000 Crossover to potential energy landscape dominated dynamics in a model glass-forming liquid *J. Chem. Phys.* **112** 9834–40
[46] Angelani L, Di Leonardo R, Ruocco G, Scala A and Sciortino F 2000 Saddles in the energy landscape probed by supercooled liquids *Phys. Rev. Lett.* **85** 5356–9
[47] Broderix K, Bhattacharya K K, Cavagna A, Zippelius A and Giardina I 2000 Energy landscape of a Lennard-Jones liquid: statistics of stationary points *Phys. Rev. Lett.* **85** 5360
[48] Cugliandolo L F, Kurchan J and Peliti L 1997 Energy flow, partial equilibration and effective temperatures in systems with slow dynamics *Phys. Rev.* E **55** 3898
[49] Berthier L, Barrat J-L and Kurchan J 2000 A two-time-scale, two-temperature scenario for nonlinear rheology *Phys. Rev.* E **61** 5464
[50] Dyre J C 2024 Solid-that-flows picture of glass-forming liquids *J. Phys. Chem. Lett.* **15** 1603–17
[51] Guan P, Chen M and Egami T 2010 Stress-temperature scaling for steady-state flow in metallic glasses *Phys. Rev. Lett.* **104** 205701
[52] 2023 P10 beamline (available at: https://photon-science.desy.de/facilities/petra_iii/beamlines/p10_coherence_applications)